Molecular Pharmacology Fast Forward. Published on October 13, 2015 as DOI: 10.1124/mol.115.100339
This article has not been copyedited and formatted. The final version may differ from this version.

Interdicting G_q activation in airway disease by receptor-dependent and receptor-independent mechanisms*

Richard Carr III, Cynthia Koziol-White, Jie Zhang, Hong Lam, Steven S. An, Gregory G. Tall, Reynold A. Panettieri, Jr., and Jeffrey L. Benovic

Department of Biochemistry and Molecular Biology, Thomas Jefferson University, Philadelphia, PA 19107, RC III, JLB
Department of Medicine, Pulmonary, Allergy and Critical Care Division, Airways Biology Initiative, University of Pennsylvania Perelman School of Medicine, Philadelphia, PA 19104, CKW, JZ, RAP Jr.
Department of Environmental Health Sciences, Johns Hopkins Bloomberg School of Public Health, Baltimore, MD 21205, HL, SSA
Department of Pharmacology and Physiology, University of Rochester Medical Center, Rochester, NY 14642, GGT

Molecular Pharmacology Fast Forward. Published on October 13, 2015 as DOI: 10.1124/mol.115.100339
This article has not been copyedited and formatted. The final version may differ from this version.

Running title: Interdicting G_q activation in airway disease

Correspondence: Jeffrey L. Benovic, Ph.D.,
Department of Biochemistry and Molecular Biology
Thomas Jefferson University
233 S. 10th St., 926 BLSB
Philadelphia, PA 19107
Tel.: 215-503-4607
E-mail: jeffrey.benovic@jefferson.edu

Number of text pages: 35

Number of tables: 0

Number of figures: 4

Number of words in Abstract: 221

Number of words in Introduction: 525

Number of words in Discussion: 1498

Abbreviations: β_2AR, β_2-adrenergic receptor; ASM, airway smooth muscle; cAMP, 3'-5'-cyclic adenosine monophosphate; CXCR, CXC chemokine receptor; DPBS, Delbecco's phosphate buffered saline; EC_{50}, half maximal effective concentration; fsk, forskolin; DTT, dithiothreitol; $G_{12/13}$, $G\alpha_{12/13}\beta\gamma$ heterotrimer; G_i, $G\alpha_i\beta\gamma$ heterotrimer; GPCR, G protein-coupled receptor; GRK, G protein-coupled receptor kinase; G_s, $G\alpha_s\beta\gamma$ heterotrimer; GST, glutathione S-transferase; G_q, $G\alpha_q\beta\gamma$ heterotrimer; GTPγS, guanosine 5'-O-[gamma-thio]triphosphate; IBMX, 3-isobutyl-1-methylxanthine; IC_{50}, half maximal inhibitory concentration; iso, isoproterenol; PAR, protease activated receptor; PCLS, precision cut lung slice; PI3K, phosphatidylinositol-3-kinase; PDK1, phosphoinositide-dependent kinase-1; PTX, pertussis toxin; RBD, Rhotekin Rho binding domain; SDS-PAGE, sodium dodecyl sulfate-polyacrylamide gel electrophoresis; TXA_2R, thromboxane A2 receptor

Molecular Pharmacology Fast Forward. Published on October 13, 2015 as DOI: 10.1124/mol.115.100339
This article has not been copyedited and formatted. The final version may differ from this version.

Abstract

G_q, an important mediator in the pathology of airway disease, plays a central role in bronchoconstriction and airway remodeling including airway smooth muscle (ASM) growth and inflammation. Current therapeutic strategies to treat airway disease include the use of muscarinic and leukotriene receptor antagonists; however, these pharmaceuticals demonstrate a limited clinical efficacy as multiple G_q-coupled receptor subtypes contribute to these pathologies. Thus, broadly inhibiting the activation of G_q may be an advantageous therapeutic approach. Here, we investigated the effects of broadly inhibiting G_q activation *in vitro* and *ex vivo* using receptor-dependent and receptor-independent strategies. P4pal-10 is a PAR4-derived pepducin that exhibits efficacy towards multiple G_q-coupled receptors. Mechanistic studies demonstrated that P4pal-10 selectively inhibits all G protein coupling to several G_q-coupled receptors including PAR1, muscarinic acetylcholine M3 and histamine H1 receptors while demonstrating no direct effect on G_q. We also evaluated the ability of FR900359, also known as UBO-QIC, to directly inhibit G_q activation. FR900359 inhibited spontaneous $G\alpha_q$ nucleotide exchange while having little effect on G_s, G_i or $G_{12/13}$ activity. Both P4pal-10 and FR900359 inhibited G_q-mediated intracellular signaling and primary human ASM growth while only FR900359 effectively interdicted agonist-promoted airway contraction in human precision cut lung slices. These studies serve as proof-of-concept that the broad-based inhibition of G_q activation may be a useful therapeutic approach to treat multiple common pathologies of airway disease.

Molecular Pharmacology Fast Forward. Published on October 13, 2015 as DOI: 10.1124/mol.115.100339
This article has not been copyedited and formatted. The final version may differ from this version.

Introduction

Asthma manifests as a complex respiratory syndrome of airway hyperesponsiveness and inflammation. Airway smooth muscle (ASM) shortening evokes airway obstruction that clinically manifests as a significant decrease in peak airflow (Deshpande and Penn, 2006). Common therapeutic interventions include the use of glucocorticoids to curb airway inflammation and are often combined with a long-acting β-agonist. Other therapies include leukotriene and muscarinic receptor antagonists that inhibit the activation of G_q-coupled receptors that mediate parasympathetic and hormonal signaling regulating bronchomotor tone (Bel, 2013). GPCR antagonists have somewhat limited efficacy in patients as the activation of multiple G_q-coupled receptors contribute to the pathology of the disease (Moulton and Fryer, 2011; Scadding and Scadding, 2010). It is plausible that inhibiting G_q activation at the receptor or the G protein level would be an advantageous asthma therapeutic as G_q-mediated ASM shortening is a primary contributor to bronchotone (Borchers et al., 2003; Pelaia et al., 2008).

P4pal-10 is a pepducin antagonist derived from intracellular loop 3 of protease-activated receptor 4 (PAR4) (Covic et al., 2002). In the initial report, P4pal-10 demonstrated efficacy in preventing PAR4-mediated platelet activation *ex vivo* and exhibited anti-thrombotic activities *in vivo*. Interestingly, P4pal-10 inhibited both PAR1- and PAR4-mediated platelet aggregation and it was suggested this was due to disruption of the activity of PAR1/PAR4 heterodimers and loss of responsiveness from both receptor subtypes. Moreover, while Covic et al. reported that P4pal-10 had little effect on thromboxane A2 receptor (TXA_2R) function in platelets (Covic et al, 2002), other investigators reported that TXA_2R was sensitive to P4pal-10 in human platelet aggregation at concentrations comparable to those used to inhibit PAR1 and PAR4 (Stampfuss et al., 2003). Here, we further investigated the putative multiple efficacies of P4pal-10 and applied

Molecular Pharmacology Fast Forward. Published on October 13, 2015 as DOI: 10.1124/mol.115.100339
This article has not been copyedited and formatted. The final version may differ from this version.

its unique properties to understand mechanisms and application of broad-based G_q inhibition in the treatment of airway disease.

The relative therapeutic advantage of broad-based G_q inhibition was also studied using a small molecule inhibitor of G_q activation, FR900359 (also known as UBO-QIC). FR900359 is a cyclic depsipeptide isolated from the roots of *Ardisia crenatasims* that is nearly structurally identical to the well-studied G_q inhibitor YM-254890 (Fujioka et al., 1988; Taniguchi et al., 2003, Takasaki et al., 2004; Bernard et al., 2014). Although not as well-characterized as YM-254890, FR900359 likely retains the same properties and mode of operation. Structural studies of a YM-254890/$G\alpha_q$ complex revealed that the compound interacts with the hinge region between the α-helical domain and GTPase domain of $G\alpha_q$ (Nishimura et al., 2010). These contacts may inhibit the opening of the nucleotide binding pocket that is requisite for GDP/GTP exchange and subsequent G protein activation. Recent studies using FR900359 demonstrate efficacy in inhibiting G_q-mediated signaling in human platelets with little effect on the activity of G_s, G_i or $G_{12/13}$ (Inamdar et al., 2015). Further, the proposed vasorelaxant properties were confirmed in an *ex vivo* model of rat aortic relaxation (Zaima et al., 2013). FR900359 has also been used as a molecular tool to dissect cellular signaling pathways that include the influence of Gβ5-RGS7 complex formation on G_q-mediated calcium flux (Karpinsky-Semper et al., 2014). Here, we assessed the ability of FR900359 to inhibit G_q-dependent airway smooth muscle growth and airway contraction.

Materials and Methods

Materials- P4pal-10 (palmitate-SGRRYGHALR-amide), scrambled P4pal-10 (P4pal-10 Scr, palmitate-YLHARGSRGR-amide) and PAR1-agonist peptide (PAR1-AP, SFLLRN) were

Molecular Pharmacology Fast Forward. Published on October 13, 2015 as DOI: 10.1124/mol.115.100339
This article has not been copyedited and formatted. The final version may differ from this version.

synthesized by an Fmoc solid-phase protocol and purified to >98% by C18 reverse-phase chromatography (Peptide2.0). FR900359 was acquired under the name of UBO-QIC from the Pharmazeutische Biologie at the Universität Bonn. Pertussis toxin from Bordetella pertussis, adenosine 5′-triphosphate disodium salt hydrate (99%), bradykinin (RPPGFSPFR) acetate salt (99%), forskolin from *Coleus forskohlii* (≥ 98%), (-)-isoproterenol hydrochloride (≥ 98%) and histamine (≥ 97%) were purchased from Sigma-Aldrich. Carbamylcholine chloride (carbachol, 99%) was purchased from Acros Organics. Purified recombinant human SDF-1α was obtained from ProSpec.

Cell Culture- HEK293 and HeLa cells were cultured in Dulbecco's Modified Eagle Medium (DMEM, Cellgro) supplemented with 10% fetal bovine serum (FBS). Primary human airway smooth muscle cells were isolated from donors with no known chronic illness or medication use as previously described (Panettieri et al., 1989). Passages 4 to 7 ASM cells were maintained in complete medium (Ham's F-12 medium supplemented with 10% FBS, 25 mM HEPES, pH 7.2, 1.7 mM $CaCl_2$, 2 mM L-glutamine, 0.2 units/ml of penicillin, and 100 μg/ml streptomycin). The use of human ASM cells does not constitute human subjects research as all donor tissue is harvested anonymously and de-identified. All cells were maintained at 37 ℃ in a humidified 5% CO_2 incubator. Cells were untransfected unless specifically noted.

Calcium Mobilization- Calcium mobilization was performed as previously described with slight modifications (Luo et al., 2008). HEK293 cells or primary human ASM cells were grown to confluence in 15 cm dishes. Cells were treated with CellStripper (CellGro), washed and concentrated to $5x10^6$ cells/mL in Hank's Balanced Salt Solution (HBSS, CellGro) with 0.025% BSA. Fura2-AM (Life Technologies) dye was added to 2 μM, gently rocked and incubated for 45 min at 37 °C. Cells were pelleted by centrifugation and the supernatant was replaced with 5 mL

Molecular Pharmacology Fast Forward. Published on October 13, 2015 as DOI: 10.1124/mol.115.100339
This article has not been copyedited and formatted. The final version may differ from this version.

of HBSS and incubated at room temperature for 15 min to allow Fura2-AM processing. Cells were pelleted by centrifugation, washed and resuspended at $30x10^6$ cells/mL in ice-cold HBSS with 0.025% BSA. To measure calcium mobilization, 50,000 cells were incubated in HBSS without calcium and magnesium (Cellgro) with 0.025% BSA in the presence or absence of various concentrations of P4pal-10 for 1 min at 37 °C. Cells treated with FR900359 were incubated on ice for 10 min before addition to the assay cuvette and 1 min incubation at 37 °C before addition of agonists (final concentrations: 100 μM PAR1-AP, 100 μM carbachol, 100 nM bradykinin, 100 μM histamine, 10 μM ATP; concentrations that promoted maximal calcium mobilization were used). Fura2-AM fluorescence was monitored using excitation at 340 and 380 nm and emission at 510 nm over a time course (LS55; PerkinElmer). Percent responsiveness was calculated as the fraction of peak response of the inhibitor treated cells as compared to the response of the cognate ligand using cells not treated with inhibitor.

G_s activation- HEK293 cells were plated in 24-well plates and grown to confluence in complete media. Before assaying, cells were treated with DMSO (0.5%), 100 nM FR900359, 10 μM P4pal-10 or 10 μM P4pal-10 Scr for 10 min at 37 °C. Cells were stimulated with 100 nM isoproterenol for 10 min in the presence of 0.5 mM 3-isobutyl-1-methylxanthine (IBMX, Sigma-Aldrich). Cells were lysed by the addition of 80 μL 0.1 M HCl followed by a 20 min incubation on an orbital shaker at room temperature. Lysates were cleared by centrifugation at 1,000 x g for 10 min. cAMP levels were measured using the Cayman Chemical Cyclic AMP EIA kit following the manufacturer's instructions. Responsiveness was calculated as a percent of isoproterenol-promoted cAMP produced as compared to the DMSO-treated cells.

G_i activation- HEK293 cells were plated in 24-well plates and grown to confluence in complete media. Before assaying, cells were treated with DMSO (0.5%), 100 nM FR900359, 10

Molecular Pharmacology Fast Forward. Published on October 13, 2015 as DOI: 10.1124/mol.115.100339
This article has not been copyedited and formatted. The final version may differ from this version.

μM P4pal-10 or 10 μM P4pal-10 Scr for 10 min at 37 °C. In pertussis toxin treated samples, cells were preincubated overnight with 100 ng/ml pertussis toxin at 37 °C. Cells were treated for 1 min with agonist (50 nM SDF-1α for CXCR4 experiments; 100 μM PAR1-AP for PAR1 experiments) before stimulation with 10 μM forskolin for 10 min. cAMP production was measured as described above. Responsiveness was calculated as a percent of forskolin-promoted cAMP produced as compared to the DMSO-treated cells.

$G\alpha_q$ purification- Rat $G\alpha_q$ and Glutathione-S-Transferase (GST)-tagged Ric-8A were co-expressed from amplified, recombinant baculoviruses (2 ml and 8 ml, respectively) in 1L of High-Five (Invitrogen) insect cell suspension culture for 48 h. Insect cells were harvested and lysed in 20 mM HEPES, pH 8.0, 150 mM NaCl, 5 mM EDTA, 1 mM dithiothreitol (DTT), 11 mM CHAPS, 1 μM GDP, and protease inhibitor mixtures, as described (Chan et al., 2011a). GST-Ric-8A:$G\alpha_q$ complexes were captured from the clarified lysates with glutathione Sepharose 4B (GE Healthcare). The column was washed and $G\alpha_q$ was eluted slowly at 22 ºC with 20 mM HEPES, pH 8.0, 50 mM $MgCl_2$, 1 mM DTT, 11 mM CHAPs, 100 μM GDP, 10 mM NaF, 30 μM $AlCl_3$, and protease inhibitor mixtures. The $G\alpha_q$ was loaded onto a 1 ml Hi-Trap Q column (GE Healthcare) that had been equilibrated with 20 mM HEPES, pH 8.0, 1 mM EDTA, 1 mM DTT, 11 mM CHAPS, and eluted with a linear gradient to 500 mM NaCl in the same buffer. The $G\alpha_q$ Hi-Trap Q pool was concentrated using an Amicon Ultra-15 30,000 MWCO ultracentrifugal device and gel filtered over a Superdex 200 HR10/300 column in 20 mM HEPES, pH 8.0, 100 mM NaCl, 1 mM EDTA, 1 mM DTT, 11 mM CHAPS, 1 μM GDP. The $G\alpha_q$ was evaluated for purity by Coomassie-stained SDS-PAGE and for activity using a Ric-8A-stimulated [^{35}S]-GTPγS binding assay (Chan et al., 2011b).

Molecular Pharmacology Fast Forward. Published on October 13, 2015 as DOI: 10.1124/mol.115.100339
This article has not been copyedited and formatted. The final version may differ from this version.

Spontaneous GTPγS binding- Intrinsic $G\alpha_q$ GTPγS binding measurements were performed as described (Nishimura et al., 2010). In brief, purified $G\alpha_q$ (500 nM) was preincubated with DMSO (0.5%), P4pal-10 or FR900359 for 5 min at 20°C in assay buffer (50 mM HEPES, pH 7.5, 1 mM EDTA, 1 mM DTT, 0.9 mM $MgSO_4$, and 0.05% Lubrol). Reactions were initiated by the addition of 10 μM [^{35}S]-GTPγS (Perkin Elmer) and 300 mM $(NH_4)_2SO_4$. The reactions were stopped by the addition of 4 mL of ice-cold wash buffer (20 mM Tris-HCl, pH 7.5, 100 mM NaCl, and 2 mM $MgSO_4$) and the $G\alpha_q$ was captured by rapid filtration through BA85 nitrocellulose membranes (Millipore). The membranes were washed four times with 4 mL of ice-cold wash buffer and [^{35}S]-GTPγS binding was quantitated by liquid scintillation counting.

Detection of active RhoA- Glutathione S-Transferase-Rhotekin Rho Binding Domain (GST-RBD, a generous gift from Dr. Philip Wedegaertner, Thomas Jefferson University) was expressed in *E. Coli* BL21 cells grown at 37 °C in 100 μg/mL ampicillin until an optical density reading at 600 nm was approximately 0.6 AU. Protein expression was induced by the addition of 0.5 mM (final concentration) isopropyl β-D-1-thiogalactopyranoside (IPTG) and continued for 3 hr at 30 °C. Cells were pelleted by centrifugation at 5000 x g for 15 min at 4 °C and resuspended in 10 mL of STE buffer (10 mM Tris-HCl, pH 8.0, 100 mM NaCl, 1 mM EDTA and 1 Complete protease inhibitor tablet (Roche)). 100 μL of 1 M DTT and 1.4 mL of 10% Sarkosyl were added and mixed by inversion. The resuspension was sonicated for 1 min and centrifuged at 18,000 x g for 30 min at 4 °C. 4 mL of 10% Triton X-100 was added to the supernatant and the solubilized mixture was supplemented with STE buffer to 20 mL. 1 mL of Glutathione Sepharose beads, pre-equilibrated with Delbecco's phosphate buffered saline (DPBS), was added to the cleared lysate. GST-RBD loading occurred over a 1 hr incubation at room temperature with gentle

Molecular Pharmacology Fast Forward. Published on October 13, 2015 as DOI: 10.1124/mol.115.100339
This article has not been copyedited and formatted. The final version may differ from this version.

rocking. Glutathione Sepharose beads were pelleted and washed 3 times with 50 mL of DPBS. Washed beads were suspended in DPBS, snap-frozen and stored at -80 °C.

HeLa cells were grown in 6-well plates to 60% confluence and transfected with FLAG-PAR1 for 48 hr prior to experiment using X-tremeGENE 9. Transfected HeLa cells were washed with DPBS and serum starved in DMEM for 4 hr at 37 °C. 10 min before stimulation, 10 μM P4pal-10, 100 nM FR900359 or 0.5% DMSO was added to the appropriate wells. After incubation, cells were stimulated with 100 μM PAR1-AP for 5 min at 37 °C. On ice, stimulation media was removed and cells were lysed with 200 μL of lysis buffer (50 mM Tris-HCl, pH 7.5, 500 mM NaCl, 0.1% sodium dodecyl sulfate (SDS), 0.5% deoxycholate, 1% Triton X-100, 20 mM $MgCl_2$ and 1 complete mini protease inhibitor tablet (Roche)). Cells were scraped, briefly sonicated on ice, and centrifuged at 1,000 x g for 10 min at 4 °C. 5 μL of each lysate was saved for total RhoA analysis. Equal protein from each lysate was incubated with 40 μg of GST-RBD for 1 hr at 4 °C. The beads were pelleted by centrifugation and washed twice with buffer (25 mM Tris-HCl, pH 7.5, 40 mM NaCl, 30 mM $MgCl_2$ and 1 complete mini protease inhibitor tablet). Bound RhoA was eluted with 2x Laemelli buffer. Proteins were separated by SDS-PAGE on a 10% polyacrylamide gel and activated RhoA pull-down was analyzed by western blotting. RhoA was detected using a monoclonal RhoA antibody (1:1000, Santa Cruz Biotechnologies) in Tris buffered saline with Tween-20 (20 mM Tris-HCl, pH 7.5, 150 mM NaCl and 0.1% Tween-20) (TBST) plus 5% BSA. Equal protein loading and RhoA expression was confirmed by blotting for RhoA after SDS-PAGE analysis of the initial lysates. For detection, western blots were incubated for 1 h at room temperature with goat anti-mouse IRDye 800 conjugated (LI-Cor Biosciences) antibodies at 1:2000. Detection of fluorescence was performed using an ODYSSEY infrared imaging system (LI-Cor Biosciences).

Molecular Pharmacology Fast Forward. Published on October 13, 2015 as DOI: 10.1124/mol.115.100339
This article has not been copyedited and formatted. The final version may differ from this version.

Airway smooth muscle growth- Primary human airway smooth muscle cells were plated at a density of 10,000 cells per well on a 96-well white opaque plate pre-coated with poly-L-lysine in complete media. After 24 hr, the complete media was removed and the cells were washed once with DPBS. Each well was supplemented with 100 μL of media (Ham's F12 medium, 25 mM HEPES, 1.7 mM $CaCl_2$, 2 mM L-Glutamine, 0.2 units/ml of penicillin, 100 μg/ml streptomycin, 5 μg/mL apo-transferrin, 1 μM insulin and 100 μM ascorbic acid) and incubated for 48 hr at 37 °C. The media was removed and cells were incubated with DMSO (0.5%), 10 μM P4pal-10, or 100 nM FR900359 for 30 min in serum-free ASM media (Ham's F12 medium, 25 mM HEPES, 1.7 mM $CaCl_2$, 2 mM L-Glutamine, 0.2 units/ml of penicillin, and 100 μg/ml streptomycin). At 30 min, cells were treated with vehicle (serum-free ASM media), 1 U/mL thrombin, 10 nM epidermal growth factor (EGF, Sigma-Aldrich), or a thrombin/EGF combination for 24 hr. Media was then removed and each well was incubated with 100 μL of WFI water (Cellgro) for 1 hr at 37 °C. 100 μL of 2x Pico Green Mix (Invitrogen) was added to each well and cells were incubated in the dark for 1 hr at room temperature. Pico Green fluorescence was excited at 485 $\pm$ 20 nm and emission was monitored at 515 $\pm$ 25 nm on a Tecan Infinite F500 microplate reader.

AKT phosphorylation- Primary human ASM cells were grown to 70-80% confluence in 6-well plates in complete media. Cells were starved for 24 hr in serum free media. 10 min prior to stimulation, cells were treated with DMSO (0.5%), 10 μM P4pal-10, or 100 nM FR900359. Cells were stimulated with vehicle (serum-free ASM media), 1 U/mL thrombin, 10 nM EGF or a thrombin/EGF combination for 6 hr at 37 °C. On ice, cells were lysed by the addition of 200 μL of lysis buffer (20 mM HEPES, pH 7.2, 150 mM NaCl, 10 mM EDTA, 1% Triton X-100 and 1 Complete protease inhibitor tablet) and brief sonication. 5x Laemelli buffer was added and

Molecular Pharmacology Fast Forward. Published on October 13, 2015 as DOI: 10.1124/mol.115.100339
This article has not been copyedited and formatted. The final version may differ from this version.

samples were boiled for 5 min. Samples were separated by SDS-PAGE on a 10% polyacrylamide gel and AKT phosphorylation was analyzed by western blotting. AKT phosphorylation was detected using a phosphospecific antibody (1:1000) against AKT phospho-serine 473 (pS^{473}, Cell Signaling Technology) in TBST with 5% BSA. Equal AKT expression was confirmed by stripping the blot and reprobing using rabbit polyclonal anti-AKT (Cell Signaling Technology), at 1:1000 in TBST with 5% BSA. For detection, western blots were incubated for 1 h at room temperature with both goat anti-rabbit IRDye 680 conjugated (LI-Cor Biosciences) and goat anti-mouse IRDye 800 conjugated (LI-Cor Biosciences) antibodies at 1:2000. Detection of fluorescence was performed using an ODYSSEY infrared imaging system (LI-Cor Biosciences).

Preparation of precision cut lung slices- Human precision cut lung slices (PCLS) were prepared from donor lungs unsuitable for transplantation in accordance with the Institutional Review Board at the University of Pennsylvania as previously described (Cooper and Panettieri, 2008; Cooper et al., 2011). Briefly, whole human lungs from non-asthma donors with no known chronic illness or medication use were dissected and inflated using 2% (wt/vol) low melting point agarose. Once the agarose set, the lobe was sectioned, and cores of 8-mm diameter were made. The cores that contained a small airway by visual inspection were sliced at a thickness of 350 μm (Precisionary Instruments VF300 Vibratome, Greenville, NC) and collected in wells containing supplemented Ham's F-12 medium. Suitable airways (≤1-mm diameter) on slices were selected on the basis of the following criteria: presence of a full smooth muscle wall, presence of beating cilia, and unshared muscle walls at airway branch points to eliminate possible counteracting contractile forces. Each slice contained ~98% parenchyma tissue; hence, all airways situated on a slice had sufficient parenchymal tissue to impart basal tone. Adjacent

Molecular Pharmacology Fast Forward. Published on October 13, 2015 as DOI: 10.1124/mol.115.100339
This article has not been copyedited and formatted. The final version may differ from this version.

slices containing contiguous segments of the same airway were paired and served as controls and were incubated at 37°C in a humidified air-CO_2 (95-5%) incubator. Sections were placed in fresh media every 2-3 hr during the remainder of *day 1* and all of *day 2* to remove agarose and endogenous substances released that variably confound the production of inflammatory mediators and/or alter airway tone.

Precision cut lung slice bronchoconstriction measurements- To assess luminal area, lung slices were placed in a 12-well plate in media and held in place using a platinum weight with nylon attachments. The airway was located using a microscope (Nikon Eclipse; model no. TE2000-U; magnification, ×40) connected to a live video feed (Evolution QEi; model no. 32-0074A-130 video recorder). Airway luminal area was measured using Image-Pro Plus software (version 6.0; Media Cybernetics) and represented in units of square micrometers (Cooper and Panettieri, 2008; Cooper et al., 2011). After functional studies, the area of each airway at baseline and for each dose of agonist was calculated using Image-Pro Plus software.

Lung slices were pretreated with FR900359 (0.1 or 1 μM), P4pal-10 (20 μM) or P4pal-10 Scr (20 μM) for 30 min at 37°C. Slices were then bronchoconstricted to a dose response of carbachol or histamine (10^{-8} – 10^{-4} M). Luminal area was measured and sigmoidal dose response curves generated from the data. Maximal bronchoconstriction (E_{max}), sensitivity of the airways to contractile agonist - log of the effective concentration to induce 50% bronchoconstriction (Log EC_{50}), and the integrated response to contractile agonist – area under the curve were calculated from the dose response curves generated and compared.

Magnetic twisting cytometry- Dynamic changes in cell stiffness were measured in isolated human ASM using forced motions of functionalized beads anchored to the cytoskeleton through cell surface integrin receptors, as described in detail previously (Fabry et al., 2001; An et al.,

Molecular Pharmacology Fast Forward. Published on October 13, 2015 as DOI: 10.1124/mol.115.100339
This article has not been copyedited and formatted. The final version may differ from this version.

2006; Deshpande et al., 2010). The increase or decrease in stiffness is considered an index of single-cell smooth muscle contraction and relaxation, respectively. For these studies, serum-deprived, post-confluent cultured ASM cells were plated at 30,000 cells/cm^2 on plastic wells (96-well Removawell, Immulon II, Dynetech) previously coated with type I collagen (VitroCol; Advanced BioMatrix, Inc.) at 500 ng/cm^2, and maintained in serum-free media for 24 h at 37ºC in humidified air containing 5% CO_2. These conditions have been optimized for seeding cultured cells on collagen matrix and for assessing their mechanical properties (Fabry et al., 2001; An et al., 2006; Deshpande et al., 2010). For each individual cell, baseline stiffness was measured for the first 60 sec and after drug addition stiffness was measured continuously for the next 240 sec; drug-induced changes in cell stiffness approached a steady-state level by 240 sec. Unless otherwise stated, ASM cells were pre-treated for 5 min with 3 μM pepducin. The effects of inhibitors were normalized to respective steady-state drug effects (without inhibitors).

Results

P4pal-10 is an antagonist of multiple G_q-coupled receptors. P4pal-10 is a ten amino acid pepducin derived from the third intracellular loop of PAR4 and was previously shown to inhibit G_q-signaling from PAR4, PAR1 and the TXA_2R (Covic et al., 2002; Stampfuss et al., 2003). To assess whether P4pal-10 broadly inhibits G_q signaling, we monitored agonist-promoted calcium mobilization from endogenous GPCRs in HEK293 cells and in primary human ASM cells. P4pal-10 effectively inhibits responsiveness to a number of agonists including carbachol, bradykinin, histamine and ATP, with potencies that range from 0.24 μM (bradykinin) to 7.4 μM (ATP) (Fig. 1A & B). To examine if P4pal-10 was specific for G_q-coupled GPCRs, the ability to inhibit G protein activation from the β_2AR (G_s-coupled) and CXCR4 (G_i-coupled) was also

Molecular Pharmacology Fast Forward. Published on October 13, 2015 as DOI: 10.1124/mol.115.100339
This article has not been copyedited and formatted. The final version may differ from this version.

assessed. P4pal-10 was unable to modulate cAMP production from the β_2AR (Fig. 1C) or adenylyl cyclase inhibition from CXCR4 (Fig. 1D). Thus, it appears that P4pal-10 operates through a specific subset of G_q-coupled receptors and does not act as a broad antagonist for G protein-receptor coupling.

P4pal-10 inhibits cognate G protein coupling to PAR1 while FR900359 directly inhibits G_q activation. It is plausible that P4pal-10 could operate by selectively inhibiting G_q activation in a receptor-dependent manner or by directly inhibiting activation of G_q. To dissect these potential mechanisms of action, the ability to modulate spontaneous nucleotide exchange was assessed using purified $G\alpha_q$. P4pal-10 had little effect on the rate of nucleotide exchange of $G\alpha_q$ suggesting that it does not operate by directly restraining G_q dynamics (Fig. 2A). We also evaluated the effects of the G_q inhibitor FR900359 and, as expected, FR900359 effectively inhibits GTPγS incorporation and corroborates the similarities with YM-254890.

PAR1 is a protease-activated receptor that, when stimulated by thrombin or an exogenous peptide ligand, couples to G_q, G_i and $G_{12/13}$ (Fig. 2B) (Gilchrist et al., 2001). As PAR1 couples to multiple G proteins and is sensitive to P4pal-10 (Fig. 1A), it serves as a good model to further dissect the mechanism of P4pal-10 inhibition. In a receptor-dependent model, P4pal-10 might operate by selectively inhibiting G_q coupling to PAR1 or by inhibiting cognate G_q, G_i and $G_{12/13}$ coupling to PAR1. To study the ability of P4pal-10 and FR900359 in isolation, the cognate signaling from each G protein subtype was assessed in cells. Both FR900359 and P4pal-10 can inhibit PAR1-agonist peptide (PAR1-AP) stimulated calcium mobilization, an event typically associated with G_q activation (Fig. 2C). Activation of G_i decreases cAMP production due to inhibition of adenylyl cyclase activity (Bokoch et al., 1984). PAR1-mediated G_i coupling resulted in an ~40% decrease in forskolin-stimulated cAMP production. Cells pretreated with

Molecular Pharmacology Fast Forward. Published on October 13, 2015 as DOI: 10.1124/mol.115.100339
This article has not been copyedited and formatted. The final version may differ from this version.

P4pal-10 were unable to modulate forskolin-stimulated cAMP production similarly to cells pretreated with pertussis toxin, a well-characterized inhibitor of G_i activation (Fig. 2D). The scrambled control pepducin had no effect on adenylyl cyclase inhibition while FR900359 also did not alter G_i function, as it is a G_q specific inhibitor (Fig. 2D). PAR1 also couples to $G_{12/13}$ activity that can be monitored through the detection of activated RhoA (McLaughlin et al., 2005). When active, RhoA binds GTP and undergoes a conformational change that can be detected by binding to a Rhotekin Rho Binding Domain glutathione-S-transferase fusion protein (GST-RBD). Using this assay, PAR1-AP effectively stimulated RhoA activation in HEK293 cells (Fig. 2E). Cells pretreated with P4pal-10 demonstrated a significant loss of detectable GTP-RhoA that was not observed in cells treated with FR900359 or P4pal-10 Scr (Fig. 2E). Using PAR1 as a model receptor, it appears that P4pal-10 may operate by inhibiting all cognate G protein coupling to a sensitive receptor such as PAR1, while FR900359 effectively inhibits G_q activation but does not alter receptor-stimulated activation of G_i or $G_{12/13}$.

Inhibition of G_q-activation by P4pal-10 or FR900359 effectively prevents synergistic airway smooth muscle growth. Pathophysiologic advancement of chronic asthma includes the physical occlusion of the airway lumen by remodeling mechanisms such as ASM hyperplasia/hypertrophy (Al-Muhsen et al., 2011). *In vitro* models of ASM growth using isolated primary human ASM cells have established a synergistic relationship between the growth effects of receptor tyrosine kinase ligands, such as EGF and platelet-derived growth factor, and concurrent exposure to G_q-coupled receptor ligands (Ediger and Toews, 2000; Krymskaya et al., 2000; Gosens et al., 2003; Billington et al., 2005; Kong et al., 2006). Synergistic ASM cell growth is dependent on the activation of G_q-coupled GPCRs and operates independently of G_i activation (insensitive to pertussis toxin) and $G_{12/13}$ signaling (insensitive to p115RhoGEF-

Molecular Pharmacology Fast Forward. Published on October 13, 2015 as DOI: 10.1124/mol.115.100339
This article has not been copyedited and formatted. The final version may differ from this version.

mediated $G_{12/13}$ inactivation) (Kong et al., 2006). As G_q plays a central role in this phenomenon, it is plausible that the inhibition of G_q activation could decouple the synergistic growth response from typical responsiveness to receptor tyrosine kinase-dependent growth factors. To examine this, primary human ASM cells were growth-arrested and exposed to thrombin (1 U/mL), epidermal growth factor (EGF, 10 nM) or co-treatment (thrombin + EGF) in the presence or absence of P4pal-10 or FR900359. As expected, ASM cells showed modest growth when treated with thrombin; more pronounced growth in the presence of EGF; and synergistic growth when co-treated with thrombin and EGF (Fig. 3A). FR900359 effectively inhibited the synergistic growth effect of thrombin + EGF treatment to levels comparable to EGF stimulation alone while cellular responsiveness to EGF was unaltered. P4pal-10 mirrored the pharmacological profile of FR900359 while P4pal-10 Scr had no effect on ASM growth (Fig. 3A).

The activation of G_q-coupled GPCRs leads to the activation of myriad intracellular signaling pathways that can contribute to cell growth. Interestingly, the synergy between G_q-coupled receptor agonists operates primarily through Gβγ-dependent activation of Akt and downstream targets of Akt, particularly P70 S6 kinase (P70S6K) (Ediger and Toews, 2000; Krymskaya et al., 2000; Kong et al., 2006). Inhibition of src, Rho and Rho kinase along with knockdown of β-arrestin suggests no role for these signaling pathways in synergistic ASM growth (Kong et al., 2006). Gβγ promotes AKT activation by direct phosphatidylinositol-3-kinase (PI3K) recruitment, phosphoinositide-dependent kinase-1 (PDK1) activation, and AKT-T308 phosphorylation by PDK1 (Billington et al., 2005). As for $G\alpha_q$, the signaling cascade that activates AKT is not as well established in ASM. Similar to the phenotypic growth assays, growth-arrested primary human ASM cells were treated, in the presence or absence of P4pal-10 or FR900359, with thrombin (1 U/mL), EGF (10 nM) or thrombin and EGF. Using an AKT

Molecular Pharmacology Fast Forward. Published on October 13, 2015 as DOI: 10.1124/mol.115.100339
This article has not been copyedited and formatted. The final version may differ from this version.

phosphospecific antibody detecting phosphorylation at S473, an indicator of activation, cells exhibited synergistic phosphorylation at S473 when co-stimulated with thrombin and EGF (Fig. 3B). Both FR900359 and P4pal-10 effectively inhibited synergistic responsiveness to levels comparable to cells treated with EGF alone. P4pal-10 Scr had little effect on agonist-promoted AKT phosphorylation (Fig. 3B).

FR900359, but not P4pal-10, can interdict bronchoconstriction in human precision cut lung slices. Airway hyperresponsiveness and amplified ASM shortening define the asthmatic diathesis. ASM contraction is mediated through myosin light chain phosphorylation downstream of G_q activation (Hakonarson and Grunstein, 1998). Parasympathetic stimulation of airway contraction is primarily mediated through the M_3 muscarinic acetylcholine receptor (Canning and Fischer, 2001). However, it is known that activation of multiple G_q-coupled GPCRs, including PARs and histamine receptors, can feed into the dynamics of airway contraction (Deshpande and Penn, 2006). Current therapeutic approaches may include the use of muscarinic or leukotriene receptor antagonists to attenuate the relative contribution of these receptors to the contractile state (Bel, 2013). Conceivably, due to the heterologous nature of the signaling inputs that regulate airway contraction, a molecule that inhibits multiple G_q-coupled receptors, such as P4pal-10, or a molecule that directly inhibits G_q activation, such as FR900359, may offer unique therapeutic benefits.

P4pal-10 and FR900359 inhibited the activation of G_q-dependent processes such as calcium mobilization or synergistic ASM growth. However, these assays were performed with either suspended cells or ASM cells grown in monolayer. As ASM *in situ* is situated under a layer of epithelial cells in the airway, the therapeutic potential of P4pal-10 and FR900359 in the context of a bronchial tissue was studied using human precision cut lung slices. As an *ex vivo* model of

Molecular Pharmacology Fast Forward. Published on October 13, 2015 as DOI: 10.1124/mol.115.100339
This article has not been copyedited and formatted. The final version may differ from this version.

airway dynamics, precision cut lung slices remain responsive to multiple receptor agonists and have been used to study physiological processes including airway bronchoconstriction. Preincubation with 100 nM or 1 μM FR900359 shifted the EC_{50} of carbachol-promoted airway contraction by 2- or 11-fold, respectively, and promoted a large reduction in maximal bronchoconstriction at 1 μM FR900359 (Fig. 4A & C) while P4pal-10 was ineffective at modulating contractile responsiveness to carbachol stimulation (Fig. 4B & C). Airway contraction was also assessed in response to histamine. As expected, FR900359 was able to effectively inhibit contractile responsiveness to high concentrations of histamine with EC_{50} shifts >50-fold and a large reduction in maximal bronchoconstriction (Fig. 4D & F). Interestingly, P4pal-10 shifted the EC_{50} of histamine responsiveness by 8-fold, albeit with a minimal effect on maximal bronchoconstriction, while P4pal-10 Scr had little effect on the EC_{50} (Fig. 4E & F). While it is expected that P4pal-10 would have the properties to interdict carbachol and histamine-promoted airway contraction, we observed relatively weak inhibition of these processes as compared to FR900359 (Fig. 4C & E). In the airway, the smooth muscle is situated under a layer of epithelial cells that P4pal-10 would have to bypass or transverse to access the ASM.

To more directly assess the ability of P4pal-10 to inhibit isolated ASM cell contraction, magnetic twisting cytometry was used to assay single cell contraction. P4pal-10 effectively inhibited carbachol and histamine-promoted single cell ASM contraction while having no effect on isoproterenol-promoted relaxation (Fig. 4F-H). Additionally, P4pal-10 Scr did not exhibit any significant effects on agonist-promoted single cell contraction or relaxation (Fig. 4F-H). As P4pal-10 was able to inhibit agonist-promoted contraction in isolated ASM cells but did not

Molecular Pharmacology Fast Forward. Published on October 13, 2015 as DOI: 10.1124/mol.115.100339
This article has not been copyedited and formatted. The final version may differ from this version.

exhibit similar efficacy in the PCLS model, tissue accessibility may be limiting the therapeutic efficacy of P4pal-10 in the airway.

Discussion

Asthma, a complex airway syndrome, manifests as airway hyperresponsiveness and inflammation due to multiple environmental and signaling inputs resulting in the exclusion of the airway lumen. G_q plays a central role in the pathophysiology of airway disease and mediates ASM contractility, airway remodeling and ASM cell growth (Deshpande and Penn, 2006). To assess the effects of broadly inhibiting G_q activation, we examined a receptor-dependent pepducin antagonist of G_q-activation alongside a small-molecule, direct inhibitor of G_q activation.

P4pal-10 is a pepducin antagonist derived from intracellular loop 3 of PAR4. In the initial report, P4pal-10 exhibited strong inhibition of PAR4-mediated platelet aggregation with an IC_{50} of ~ 0.5-1 μM and, interestingly, was able to also modulate PAR1-mediated platelet aggregation (Covic et al., 2002). P4pal-10 could also inhibit G_q-signaling in response to TXA_2R stimulation (Stampfuss et al., 2003), although this effect was not observed by Covic et al (Covic et al., 2002). By monitoring calcium mobilization in HEK293 and human ASM cells, P4pal-10 inhibited a number of G_q-coupled receptors with IC_{50}s ranging from 0.24-7.4 μM. As the efficacy of P4pal-10 varied greatly depending on the agonist specificity, it seems unlikely that P4pal-10 is directly sequestering G_q and preventing receptor interaction. Indeed, P4pal-10 did not modulate nucleotide exchange using purified $G\alpha_q$. An interesting property exhibited by P4pal-10 concerns the ability to interdict all G protein coupling to a single receptor. PAR1 can couple to G_q, G_i and $G_{12/13}$, all of which can be inhibited by P4pal-10. It is unknown, at this time,

Molecular Pharmacology Fast Forward. Published on October 13, 2015 as DOI: 10.1124/mol.115.100339
This article has not been copyedited and formatted. The final version may differ from this version.

if P4pal-10 operates by restricting conformational dynamics of its targeted receptors to stabilize an inactive state or if P4pal-10 prevents receptor interaction with a G protein.

As P4pal-10 appears to operate through the receptor, the mechanism in which P4pal-10 inhibits a diverse set of G_q-coupled receptors remains elusive. It was previously believed that pepducins operate through the cognate receptor from which they were derived (O' Callaghan et al., 2012); however, some pepducins, including P4pal-10, exhibit efficacy across multiple receptor subtypes (Stampfuss et al., 2003, Carr III et al., 2014). While many of these receptors do not share significant sequence similarity, many of the P4pal-10 sensitive receptors share strong, sequential homology with the N-terminal-half of the P4pal-10 sequence (SGRRYG). Some receptors that were characterized as P4pal-10 insensitive, such as the β_2AR, may share some sequence homology with P4pal-10 but these regions of similarity are either short and highly disjointed or found in receptor regions that are likely not playing a role in P4pal-10 function (extracellular loops and transmembrane domains). Further, P4pal-10 sensitive receptors exhibited sequence homology with P4pal-10 in the intracellular domains of the receptor along with some portions of transmembrane domains that border the intracellular surface. With this in mind, P4pal-10 may interrupt critical intra-receptor or receptor-G protein contacts that are necessary for agonist-promoted G protein activation. As each receptor has distinct differences in receptor sequence, the spectrum of P4pal-10 sensitivity (Fig. 1A & B) may be attributed to the degree of similarity between the receptor and P4pal-10 or the unknown P4pal-10 interaction site.

FR900359, also known as UBO-QIC, was first reported as a methanol-extracted natural compound isolated from *Ardisia crenata sims* that was proposed to inhibit *in vitro* platelet aggregation and decrease blood pressure in rats (Fujioka et al., 1988). Similar to the well-studied YM-254890, FR900359 directly inhibited *in vitro* spontaneous nucleotide exchange using

Molecular Pharmacology Fast Forward. Published on October 13, 2015 as DOI: 10.1124/mol.115.100339
This article has not been copyedited and formatted. The final version may differ from this version.

purified $G\alpha_q$ which suggests that it is operating by constraining G_q conformational dynamics. Our studies confirmed the proposed specificity of the compound at concentrations ten-times higher than concentrations previously studied *in vitro*. FR900359 did not modulate G_s, G_i or $G_{12/13}$ signaling while strongly inhibiting G_q activation (Inamdar et al, 2015). As many GPCRs couple to multiple G proteins, the use of an inhibitor with defined specificity can effectively bias signaling from a GPCR. Most often studied is the ability of a GPCR agonist to promote a biased signal but FR900359 promotes an inhibitor-biased signal by selectively eliminating the activation of a particular intracellular signaling protein. Using PAR1, for example, FR900359 effectively eliminated G_q activation from PAR1 while allowing activation of G_i and $G_{12/13}$ from the same receptor. Thus, FR900359 changed PAR1 signaling from G_q, G_i and $G_{12/13}$ to only G_i and $G_{12/13}$. The concept of inhibitor biased signaling can be applied to a number of kinase inhibitors (e.g., G protein-coupled receptor kinase (GRK), PKA, PKC, etc) or molecular inhibitors (pertussis toxin, Rho inhibitors, etc.) to modulate the lifetime (kinetics) or efficacy of signaling and, thus, provide a new dimension to biasing intracellular signaling pathways.

Investigation into the molecular mechanisms of airway disease clearly demonstrates a central role for G_q activation and downstream signaling. Most prominently in patients with asthma, hyperresponsiveness of ASM by phosphorylation of myosin light chain is, in part, a downstream consequence of G_q-promoted calcium mobilization (Hakonarson and Grunstein, 1998). Although the mechanism of elevated G_q-signaling remains incompletely understood, it is believed that increased parasympathetic activation of the airway along with a local increase in G_q-coupled receptor agonists (e.g., thrombin, histamine, ATP) enhances contractile state of an asthmatic airway. It is suspected that both inputs contribute to the pathology as muscarinic antagonists only partially alleviate airway tension in patients (Bel, 2013). Using *ex vivo* human precision cut lung

Molecular Pharmacology Fast Forward. Published on October 13, 2015 as DOI: 10.1124/mol.115.100339
This article has not been copyedited and formatted. The final version may differ from this version.

slices, direct inhibition of G_q activation by FR900359 was able to significantly impact airway contraction. Thus, it is conceivable that the use of a G_q specific inhibitor may be an advantageous approach to the complex nature of treating bronchoconstriction in the asthmatic airway.

G_q also contributes to airway remodeling, including ASM growth, that physically occlude the lumen of the airway (Al-Muhsen, 2011). ASM proliferation is exacerbated in the disease state due to multiple factors including the increased presence of G_q-coupled receptor agonists such as histamine, acetylcholine, thromboxane, leukotriene D4, serotonin and ATP in the airway (Deshpande and Penn, 2006). *In vitro* models of ASM growth have established a synergistic relationship between the growth effects of receptor tyrosine kinase ligands, such as EGF and platelet-derived growth factor, and concurrent exposure to G_q-coupled receptor ligands that is mediated through the activation of Akt and P70S6K (Ediger and Toews, 2000; Krymskaya et al., 2000; Kong et al., 2006). Both P4pal-10 and FR900359 inhibited synergistic ASM growth and synergistic AKT activation with similar efficacy. These compounds, through fundamentally different mechanisms, inhibit synergy without modulating cellular responsiveness to a RTK growth factor further corroborates the critical role G_q plays in this phenomena and pathology. G_q can also promote the release of inflammatory factors such as cytokines (Fujii et al., 1998; Fujii and Kawashima, 2000). Considering the data monitoring ASM contractility and growth, it would be expected that both P4pal-10 and FR900359 may have a significant impact on the efficacy of this process.

To date, the *in vivo* efficacy of pepducins has been limited to treating diseases in which the target cell type is readily accessible. For example, PAR1- and PAR4-targeted pepducin antagonists were demonstrated to have significant efficacy in interdicting platelet thrombosis in mouse and non-human primate disease models (Covic et al., 2002; Zhang et al., 2012). In nude

Molecular Pharmacology Fast Forward. Published on October 13, 2015 as DOI: 10.1124/mol.115.100339
This article has not been copyedited and formatted. The final version may differ from this version.

mice, P1pal-7 effectively inhibited epithelial-derived lung tumor formation comparably to the current therapeutic standard Bevacizumab (Cisowski et al., 2011). A CXCR2 pepducin antagonist inhibited inflammation and spontaneous tumor development by inhibition of CXCR2-rich leukocyte association in an invasive intestinal adenocarcinoma murine model (Jamieson et al., 2012). It should be noted that each of the targeted cell types, such as platelets and leukocytes, were primarily accessible to circulating pepducins. In a tissue, the target cell types will likely need to have a surface accessible to the bloodstream in order for pepducin delivery. As pepducins do not have a particular targeting mechanism, the hydrophobic N-terminal palmitoyl group will likely incorporate into any membrane that it comes in contact with. In a multilayered tissue, the outermost cell type, epithelial cells in the case of the airway, may act as a sink to capture much of the available pepducin. This hypothesis is corroborated by the phenomena observed while monitoring ASM signaling pathways and contraction in cell monolayer in comparison to airway contraction in an *ex vivo*, intact airway using precision cut lung slices. P4pal-10 was unable to modulate airway contraction in the airway tissue but exhibited strong efficacy in inhibiting single cell contraction using isolated ASM cells. Additionally, P4pal-10 could inhibit G_q-dependent signaling in cell suspension or monolayer. Plausibly, as the ASM is situated under an epithelial layer, P4pal-10 cannot adequately penetrate the tissue to reach the ASM. In contrast, FR900359 significantly inhibited agonist-promoted contraction in the precision cut lung slices. These observations are likely a commentary on the current therapeutic limitations of the use of pepducins to treat human disease. As previously demonstrated, pepducins can offer novel therapeutic approaches if the targeted cell type is not part of a multilayered tissue (i.e., platelets, leukocytes) or it is able to interact with bioavailable pepducin (i.e., lung epithelial tissue). Beyond therapeutic application, it is becoming increasingly clear that

Molecular Pharmacology Fast Forward. Published on October 13, 2015 as DOI: 10.1124/mol.115.100339
This article has not been copyedited and formatted. The final version may differ from this version.

pepducins, including P4pal-10, can provide unique pharmacological tools and profiles that are not currently ascertainable using orthosteric ligands.

Molecular Pharmacology Fast Forward. Published on October 13, 2015 as DOI: 10.1124/mol.115.100339
This article has not been copyedited and formatted. The final version may differ from this version.

Acknowledgements

The authors would like to thank Drs. Christopher So, Thomas Charpentier, Raymond Penn and Matthew Schiewer for valuable discussions and Christopher Fischer and Dr. Philip Wedegaertner for their advice in generating the GST-RBD beads.

Author Contributions

Participated in research design: Carr III, Koziol-White, Lam, An, Panettieri and Benovic.

Conducted experiments: Carr III, Koziol-White, Lam and Zhang.

Contributed new reagents or analytic tools: Carr III, Koziol-White, Panettieri, Tall and An

Performed data analysis: Carr III, Koziol-White, Panettieri and Benovic

Wrote or contributed to the writing of the manuscript: Carr III, Koziol-White, An, Panettieri, Tall, and Benovic

Molecular Pharmacology Fast Forward. Published on October 13, 2015 as DOI: 10.1124/mol.115.100339
This article has not been copyedited and formatted. The final version may differ from this version.

References

Al-Muhsen S, Johnson J R, and Hamid Q (2011) Remodeling in asthma. *J Allergy Clin Immunol* **128**: 451-462.

An SS, Fabry B, Trepat X, Wang N, and Fredberg JJ (2006) Do biophysical properties of the airway smooth muscle in culture predict airway hyperresponsiveness? *Am J Respir Cell Mol Biol* **35**: 55-64.

Bel EH (2013) Clinical Practice. Mild asthma. *N Engl J Med* **369**: 549-557.

Bernard R, Thach L, Kamato D, Osman N, and Little PJ (2014) Assessing the Role of Gαq/11 in Cellular Responses: An Analysis of Investigative Tools. *Clin Exp Pharmacol* **4**: 1000164.

Billington CK, Kong KC, Bhattacharyya R, Wedegaertner PB, Panettieri RA Jr, Chan TO, and Penn RB (2005) Cooperative regulation of p70S6 kinase by receptor tyrosine kinases and G protein-coupled receptors augments airway smooth muscle growth. *Biochemistry* **44**: 14595-14605.

Bokoch GM, Katada T, Northup JK, Ui M, and Gilman AG (1984) Purification and properties of the inhibitory guanine nucleotide-binding regulatory component of adenylate cyclase. *J Biol Chem* **259**: 3560-3567.

Borchers MT, Biechele T, Justice JP, Ansay T, Cormier S, Mancino V, Wilkie TM, Simon MI, Lee NA, and Lee JJ (2003) Methacholine-induced airway hyperresponsiveness is dependent on Galphaq signaling. Am *J Physiol Lung Cell Mol Physiol* **285**: L114-20.

Canning BJ, and Fischer A (2001) Neural regulation of airway smooth muscle tone. *Respir Physiol* **125**:113-127.

Carr R 3rd, Du Y, Quoyer J, Panettieri RA Jr, Janz JM, Bouvier M, Kobilka BK, and Benovic JL (2014) Development and characterization of pepducins as Gs-biased allosteric agonists. *J Biol Chem* **289**: 35668-35684.

Chan P, Gabay M, Wright FA, Kan W, Oner SS, Lanier SM, Smrcka AV, Blumer JB, and Tall GG (2011a) Purification of heterotrimeric G protein alpha subunits by GST-Ric-8 association: primary characterization of purified G alpha(olf). *J Biol Chem* **286**: 2625-2635.

Chan P, Gabay M, Wright FA, and Tall GG (2011b) Ric-8B is a GTP-dependent G protein alphas guanine nucleotide exchange factor. *J Biol Chem* **286**: 19932-19942.

Cisowski J, O'Callaghan K, Kuliopulos A, Yang J, Nguyen N, Deng Q, Yang E, Fogel M, Tressel S, Foley C, Agarwal A, Hunt S W, 3rd McMurry T, Brinckerhoff L, and Covic L (2011) Targeting protease-activated receptor-1 with cell-penetrating pepducins in lung cancer. *Am J Pathol* **179**: 513-523.

Cooper PR, and Panettieri Jr RA (2008) Steroids completely reverse albuterol-induced [beta]2-adrenergic receptor tolerance in human small airways. *J Allergy Clin Immunol* **122**: 734-40.

Cooper PR, Zhang J, Damera G, Hoshi T, Zopf DA, and Panettieri RA, Jr (2011) C-027 inhibits IgE-mediated passive sensitization bronchoconstriction and acts as a histamine and serotonin antagonist in human airways. *Allergy Asthma Proc* **32**: 359-65.

Molecular Pharmacology Fast Forward. Published on October 13, 2015 as DOI: 10.1124/mol.115.100339
This article has not been copyedited and formatted. The final version may differ from this version.

Covic L, Misra M, Badar J, Singh C, and Kuliopulos A (2002) Pepducin-based intervention of thrombin-receptor signaling and systemic platelet activation. *Nat Med* **8**: 1161-1165.

Deshpande DA, and Penn RB (2006) Targeting G protein-coupled receptor signaling in asthma. *Cell Signal* **18**: 2105-2120.

Deshpande DA, Wang WC, Mcllmoyle EL, Robinett KS, Schillinger RM, An SS, Sham JS, and Liggett SB (2010) Bitter taste receptors on airway smooth muscle bronchodilate by localized calcium signaling and reverse obstruction. *Nat Med* **16**: 1299-1304.

Ediger TL, and Toews ML (2000) Synergistic stimulation of airway smooth muscle cell mitogenesis. *J Pharmacol Exp Ther* **294**: 1076-1082.

Fabry B, Maksym GN, Butler JP, Glogauer M, Navajas D, and Fredberg JJ (2001) Scaling the microrheology of living cells. *Phys Rev Lett* **87**: 148102.

Fujii T, Yamada S, Watanabe Y, Misawa H, Tajima S, Fujimoto K, Kasahara T, and Kawashima K (1998) Induction of choline acetyltransferase mRNA in human mononuclear leukocytes stimulated by phytohemagglutinin, a T-cell activator. *J Neuroimmunol* **82**: 101-107.

Fujii T, and Kawashima K (2000) Ca2+ oscillation and c-fos gene expression induced via muscarinic acetylcholine receptor in human T- and B-cell lines. *Naunyn Schmiedebergs Arch Pharmacol* **362**: 14-21.

Fujioka M, Koda S, Morimoto Y, and Biemann K (1988) Structure of FR900359, a cyclic depsipeptide from *Ardisia-Crenata Sims*. *J Org Chem* **53**: 2820-2825.

Gilchrist A, Vanhauwe JF, Li A, Thomas TO, Voyno-Yasenetskaya T, and Hamm HE (2001) G alpha minigenes expressing C-terminal peptides serve as specific inhibitors of thrombin-mediated endothelial activation. *J Biol Chem* **276**: 25672-25679.

Gosens R, Nelemans SA, Grootte Bromhaar MM, McKay S, Zaagsma J, and Meurs H (2003) Muscarinic M3-receptors mediate cholinergic synergism of mitogenesis in airway smooth muscle. *Am J Respir Cell Mol Biol* **28**: 257-262.

Hakonarson H, and Grunstein MM (1998) Regulation of second messengers associated with airway smooth muscle contraction and relaxation. *Am J Respir Crit Care Med* **158**: S115-S122.

Inamdar V, Patel A, Manne B K, Dangelmaier C, and Kunapuli S P (2015) Characterization of UBO-QIC as a Gαq inhibitor in platelets. *Platelets*: 1-8.

Jamieson T, Clarke M, Steele C W, Samuel MS, Neumann J, Jung A, Huels D, Olson MF, Das S, Nibbs RJ, and Sansom OJ (2012) Inhibition of CXCR2 profoundly suppresses inflammation-driven and spontaneous tumorigenesis. *J Clin Invest* **122**: 3127-3144.

Karpinsky-Semper D, Volmar CH, Brothers SP, and Slepak VZ (2014) Differential effects of the Gβ5-RGS7 complex on muscarinic M3 receptor-induced Ca2+ influx and release. *Mol Pharmacol* **85**: 758-768.

Krymskaya VP, Orsini MJ, Eszterhas AJ, Brodbeck KC, Benovic JL, Panettieri RA Jr, and Penn RB (2000) Mechanisms of proliferation synergy by receptor tyrosine kinase and G protein-coupled receptor activation in human airway smooth muscle. *Am J Respir Cell Mol Biol* **23**: 546-554.

Kong KC, Billington CK, Gandhi U, Panettieri RA Jr, and Penn RB (2006) Cooperative mitogenic signaling by G protein-coupled receptors and growth factors is dependent on G(q/11). *FASEB J* **20**: 1558-1560.

Luo J, Busillo JM, and Benovic JL (2008) M3 muscarinic acetylcholine receptor-mediated signaling is regulated by distinct mechanisms. Mol *Pharmacol* **74**: 338-347.

McLaughlin JN, Shen L, Holinstat M, Brooks JD, Dibenedetto E, and Hamm HE (2005) Functional selectivity of G protein signaling by agonist peptides and thrombin for the protease-activated receptor-1. *J Biol Chem* **280**: 25048-25059.

Moulton BC, and Fryer AD (2011) Muscarinic receptor antagonists, from folklore to pharmacology; finding drugs that actually work in asthma and COPD. *Br J Pharmacol* **163**: 44-52.

Nishimura A, Kitano K, Takasaki J, Taniguchi M, Mizuno N, Tago K, Hakoshima T, and Itoh H (2010) Structural basis for the specific inhibition of heterotrimeric Gq protein by a small molecule. *Proc Natl Acad Sci USA* **107**: 13666-13671.

O'Callaghan K, Kuliopulos A, and Covic L (2012) Turning receptors on and off with intracellular pepducins: new insights into G-protein-coupled receptor drug development. *J Biol Chem* **287**: 12787-12796.

Panettieri RA, Murray RK, DePalo LR, Yadvish PA, and Kotlikoff MI (1989) A human airway smooth muscle cell line that retains physiological responsiveness. *Am J Physiol* **256**: C329-C335.

Pelaia G, Renda T, Gallelli L, Vatrella A, Busceti MT, Agati S, Caputi M, Cazzola M, Maselli R, and Marsico SA (2008) Molecular mechanisms underlying airway smooth muscle contraction and proliferation: implications for asthma. *Respir Med* **102**: 1173-1181

Scadding GW, and Scadding GK (2010) Recent advances in antileukotriene therapy. *Curr Opin Allergy Clin Immunol* **10**: 370-376.

Stampfuss JJ, Schror K, and Weber AA (2003) Inhibition of platelet thromboxane receptor function by a thrombin receptor-targeted pepducin. *Nat Med* **9**: 1447

Takasaki J, Saito T, Taniguchi M, Kawasaki T, Moritani Y, Hayashi K, and Kobori M (2004) A novel Gαq/11-selective inhibitor. *J Biol Chem* **279**: 47438-47445.

Taniguchi M, Nagai K, Arao N, Kawasaki T, Saito T, Moritani Y, Takasaki J, Hayashi K, Fujita S, Suzuki K, and Tsukamoto S (2003) YM-254890, a novel platelet aggregation inhibitor produced by *Chromobacterium sp. QS3666. J Antibiot (Tokyo)* **56**: 358-363.

Zaima K, Deguchi J, Matsuno Y, Kaneda T, Hirasawa Y, and Morita H (2013) Vasorelaxant effect of FR900359 from *Ardisia crenata* on rat aortic artery. *J Nat Med* **67**: 196-201.

Zhang P, Gruber A, Kasuda S, Kimmelstiel C, O'Callaghan K, Cox DH, Bohm A, Baleja JD, Covic L, and Kuliopulos A (2012) Suppression of arterial thrombosis without affecting hemostatic parameters with a cell-penetrating PAR1 pepducin. *Circulation* **126**: 83-91.

Molecular Pharmacology Fast Forward. Published on October 13, 2015 as DOI: 10.1124/mol.115.100339
This article has not been copyedited and formatted. The final version may differ from this version.

***Footnotes**

This research was supported by the National Institutes of Health National Institute of General Medical Sciences [Grants R37-GM047417, R01-GM068857, R01-GM088242, T32-GM100836], National Institutes of Health National Heart, Lung and Blood Institute [P01-HL114471, R01 HL107361] and National Institutes of Health National Institute of Environmental Health Sciences [P30-ES013508].

Molecular Pharmacology Fast Forward. Published on October 13, 2015 as DOI: 10.1124/mol.115.100339
This article has not been copyedited and formatted. The final version may differ from this version.

Figure Legends

Fig. 1. P4pal-10 is an antagonist of multiple G_q-coupled receptors. (A) Agonist-promoted calcium mobilization was monitored by Fura-2AM fluorescence in HEK293 and HASM cells pretreated for 1 min with various concentrations of P4pal-10. Peak fluorescence values are reported. (B) P4pal-10 IC_{50} values are reported for responsiveness to various G_q-coupled receptor agonists. (C) 10 μM P4pal-10 does not inhibit isoproterenol-stimulated cAMP production (G_s-mediated) in HEK293 cells. The data are represented by the mean ± SD from three independent experiments. ns- not significant (D) 10 μM P4pal-10 does not inhibit SDF-1α stimulated adenylyl cyclase inhibition (G_i-mediated) in HEK293 cells. The data are represented by the mean ± SD from three independent experiments. **- $p < 0.01$ versus forskolin-treated cells using a two-way unpaired t-test.

Fig. 2. P4pal-10 inhibits cognate G protein coupling to PAR1 while FR900359 directly inhibits G_q. (A) 100 nM FR900359, but not 10 μM P4pal-10, interdicts spontaneous GTPγS binding to purified $G\alpha_q$. The data are represented by the mean ± SD from three independent experiments. (B) PAR1 can couple to G_q (measured by calcium mobilization), G_i (measured by adenylyl cyclase inhibition) and $G_{12/13}$ (measured by RhoA activation). (C) 10 μM P4pal-10 and 100 nM FR900359 inhibits PAR1-AP promoted calcium mobilization. ***- $p < 0.001$ versus vehicle-treated cells using a two-way unpaired t-test. (D) 10 μM P4pal-10, but not 100 nM FR900359 or 10 μM P4pal-10 Scr, can inhibit PAR1-dependent G_i activation. P4pal-10 exhibited comparable efficacy to pertussis toxin, an inhibitor of G_i activation. The data are represented by the mean ± SD from three independent experiments. ns- not significant, **- $p < 0.01$ and ***- $p < 0.001$ versus PAR1-AP-treated cells using a two-way unpaired t-test. (E) 10 μM P4pal-10, but not 100 nM FR900359 or 10 μM P4pal-10 Scr, can inhibit PAR1-AP stimulated $G_{12/13}$ activation. The

Molecular Pharmacology Fast Forward. Published on October 13, 2015 as DOI: 10.1124/mol.115.100339
This article has not been copyedited and formatted. The final version may differ from this version.

data are represented by the mean ± SD from three independent experiments. ns- not significant, ***- p< 0.001 versus PAR1-AP-treated cells using a two-way unpaired t-test.

Fig. 3. Inhibition of G_q-activation by P4pal-10 or FR900359 effectively inhibits synergistic HASM growth and growth signaling. (A) 10 μM P4pal-10 or 100 nM FR900359, but not P4pal-10 Scr, can significantly inhibit synergistic human ASM growth in response to EGF and thrombin co-treatment while not modulating EGF-promoted cell growth. Cell growth was monitored 24 hr post-stimulation using a PicoGreen fluorescence assay. The data are represented by the mean ± SD of three independent experiments. ***- p< 0.001 versus vehicle-treated cells using a two-way unpaired t-test. (B) 10 μM P4pal-10 or 100 nM FR900359, but not P4pal-10 Scr, can significantly inhibit synergistic Akt phosphorylation at S473 in response to EGF and thrombin co-treatment while not modulating EGF-promoted phosphorylation. AKT-S473 phosphorylation was assessed by western blot six hr post-stimulation. The data are represented by the mean ± SD of three independent experiments. ns-not significant, **- p< 0.01 versus vehicle-treated cells incubated with thrombin and EGF using a two-way unpaired t-test.

Fig. 4. FR900359, but not P4pal-10, can inhibit airway contraction in human precision cut lung slices. (A) 100 nM and 1 μM FR900359 inhibited carbachol-promoted airway contraction. The data are represented by the mean $\pm$ SEM of four independent experiments and fitted to a sigmoidal dose-response model. (B) P4pal-10 and P4pal-10 Scr had no effect on airway contraction in response to carbachol. The data are represented by the mean $\pm$ SEM of four independent experiments and fitted to a sigmoidal dose-response model. The “no inhibitor” curve is derived from the same data set in both panel A and B. (C) 100 nM or 1 μM FR900359

Molecular Pharmacology Fast Forward. Published on October 13, 2015 as DOI: 10.1124/mol.115.100339
This article has not been copyedited and formatted. The final version may differ from this version.

shifted the estimated EC_{50} value of carbachol-promoted airway contraction by 2- and 11-fold, respectively. P4pal-10 and P4pal-10 Scr did not modulate carbachol responsiveness. The data are represented by the mean ± SEM of four independent experiments. ns-not significant, ***- p< 0.001 versus vehicle-treated tissue using a two-way unpaired t-test. (D) 100 nM and 1 μM FR900359 effectively inhibited histamine-promoted airway contraction. The data are represented by the mean ± SEM of three independent experiments and fitted to a sigmoidal dose-response model. (E) P4pal-10 partially inhibited airway contraction in response to histamine. The data are represented by the mean ± SEM of three independent experiments and fitted to a sigmoidal dose-response model. The "no inhibitor" curve is derived from the same data set in both panel D and E. (F) P4pal-10 shifted the estimated EC_{50} value of histamine-promoted airway contraction by 8-fold while 100 nM and 1 μM FR900359 shifted the EC_{50} >50-fold. The data are represented by the mean ± SEM of three independent experiments. ns-not significant, *- p< 0.05, **- p< 0.01 versus vehicle-treated tissue using a two-way unpaired t-test. (G) Magnetic twisting cytometry analysis of isolated ASM dynamics shows that pretreatment with 3 μM P4pal-10 (n=232) significantly inhibited carbachol-promoted single-cell contraction as compared to "no inhibitor"/vehicle treatment (n=331). P4pal-10 Scr did not exhibit similar efficacy (n=266). The data sets are normalized to "no inhibitor"/vehicle treatment. ns-not significant, ***- p< 0.001 compared to vehicle-treated cells using a one-way ANOVA analysis. (H) Magnetic twisting cytometry analysis of isolated ASM dynamics shows that pretreatment with 3 μM P4pal-10 (n=867) significantly inhibited histamine-promoted single-cell contraction as compared to "no inhibitor"/vehicle treatment (n=692). P4pal-10 Scr did not exhibit similar efficacy (n=486). The data sets are normalized to "no inhibitor"/vehicle treatment. ns-not significant, ***- p< 0.001 compared to vehicle-treated cells using a one-way ANOVA analysis. (I) Magnetic twisting

Molecular Pharmacology Fast Forward. Published on October 13, 2015 as DOI: 10.1124/mol.115.100339
This article has not been copyedited and formatted. The final version may differ from this version.

cytometry analysis of isolated ASM dynamics shows that pretreatment with 3 μM P4pal-10 (n=418) or P4pal-10 Scr (n=292) did not modulate isoproterenol-promoted single-cell relaxation as compared to “no inhibitor”/vehicle treatment (n=569). The data sets are normalized to “no inhibitor”/vehicle treatment. ns-not significant compared to vehicle-treated cells using a one-way ANOVA analysis.

A

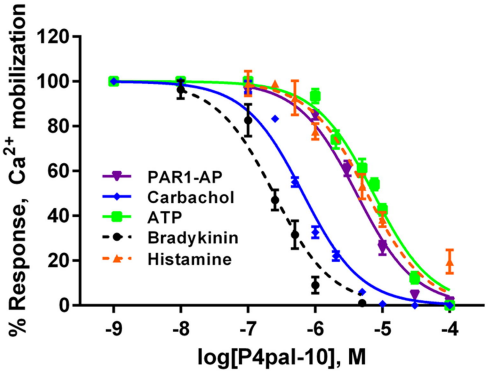

B

Agonist	Receptor	IC_{50} (μM)	Cell Type
Bradykinin	Bradykinin B2	0.24 ± 0.03	HASM
Carbachol	M3 Muscarinic	0.66 ± 0.05	HEK293
PAR1-AP	PAR1	4.10 ± 0.30	HEK293
Histamine	Histamine H1	5.87 ± 0.63	HASM
ATP	$P2Y_{1/2}$	7.36 ± 0.39	HEK293

C

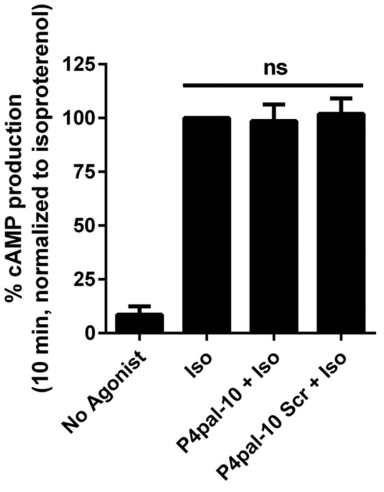

D

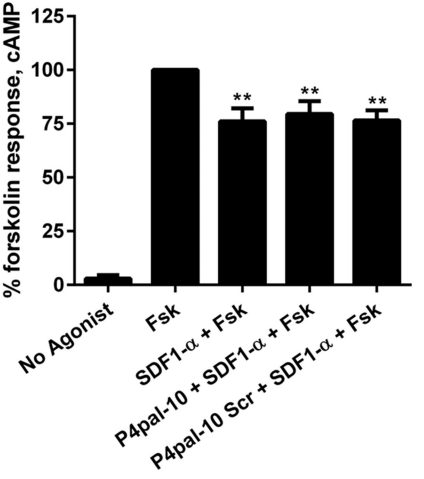

Figure 1

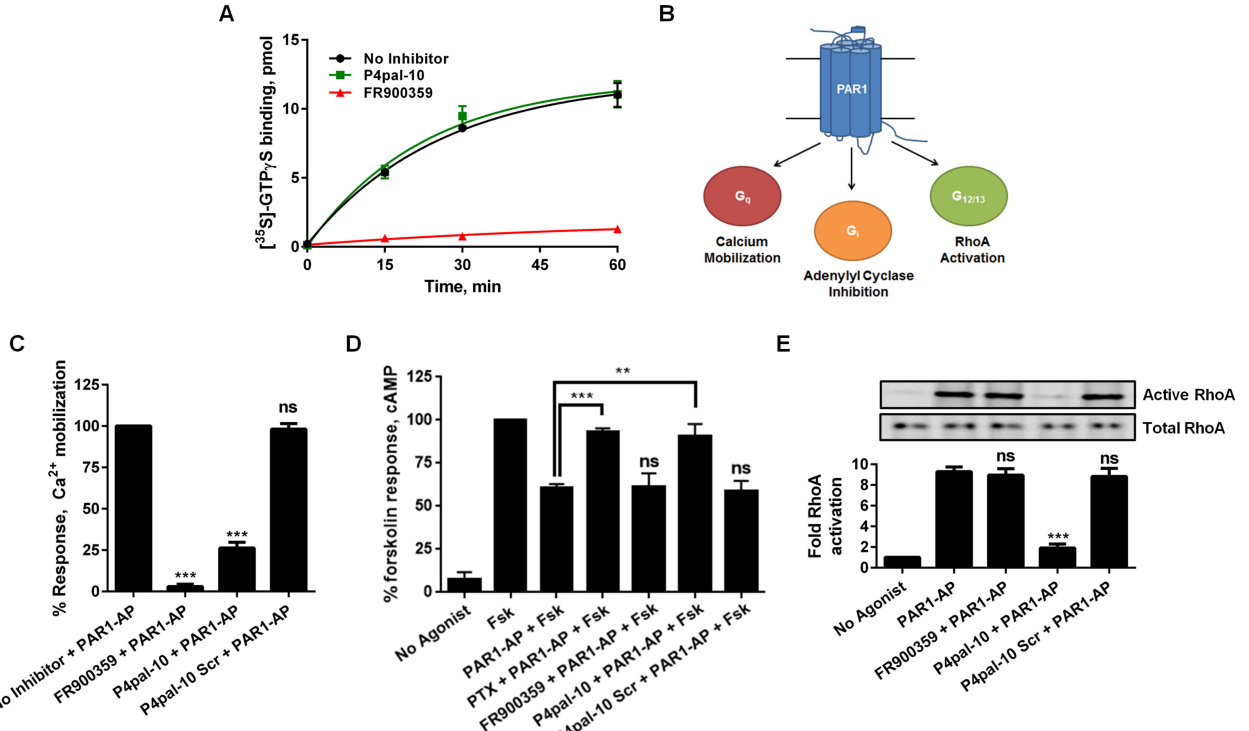
A
No Inhibitor
P4pal-10
FR900359
[35S]-GTPγS binding, pmol
Time, min
B
PAR1
Gq
G12/13
Gi
Calcium Mobilization
Adenylyl Cyclase Inhibition
RhoA Activation
C
% Response, Ca2+ mobilization
ns
***
No Inhibitor + PAR1-AP
FR900359 + PAR1-AP
P4pal-10 + PAR1-AP
P4pal-10 Scr + PAR1-AP
D
% forskolin response, cAMP
**
***
ns
No Agonist
Fsk
PAR1-AP + Fsk
PTX + PAR1-AP + Fsk
FR900359 + PAR1-AP + Fsk
P4pal-10 + PAR1-AP + Fsk
P4pal-10 Scr + PAR1-AP + Fsk
E
Active RhoA
Total RhoA
Fold RhoA activation
No Agonist
PAR1-AP
FR900359 + PAR1-AP
P4pal-10 + PAR1-AP
P4pal-10 Scr + PAR1-AP

Figure 2

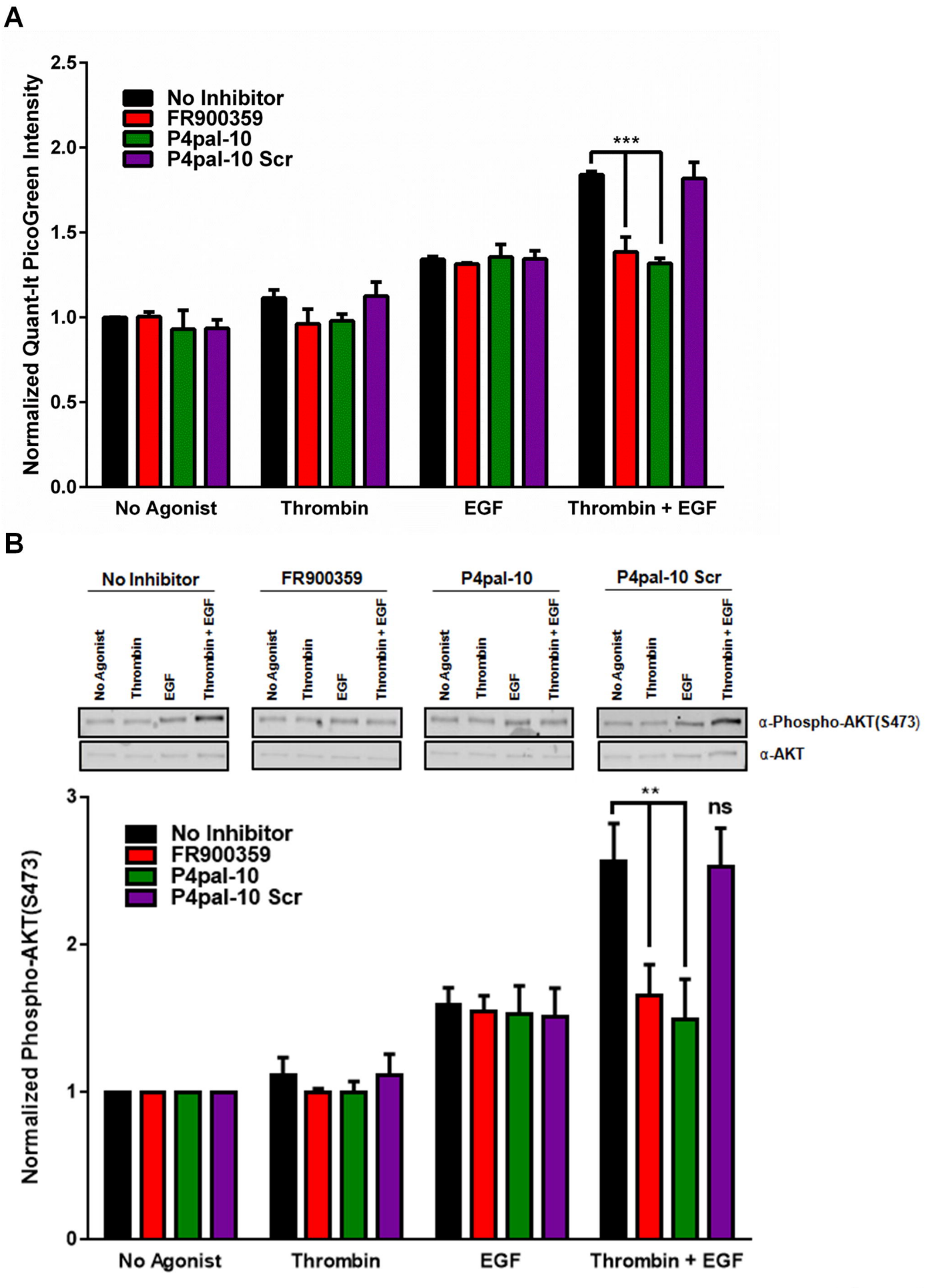
A
Normalized Quant-It PicoGreen Intensity
2.5
2.0
1.5
1.0
0.5
0.0
No Inhibitor
FR900359
P4pal-10
P4pal-10 Scr
***
No Agonist
Thrombin
EGF
Thrombin + EGF
B
No Inhibitor
FR900359
P4pal-10
P4pal-10 Scr
No Agonist
Thrombin
EGF
Thrombin + EGF
α-Phospho-AKT(S473)
α-AKT
Normalized Phospho-AKT(S473)
3
2
1
0
**
ns
No Inhibitor
FR900359
P4pal-10
P4pal-10 Scr
No Agonist
Thrombin
EGF
Thrombin + EGF

Figure 3

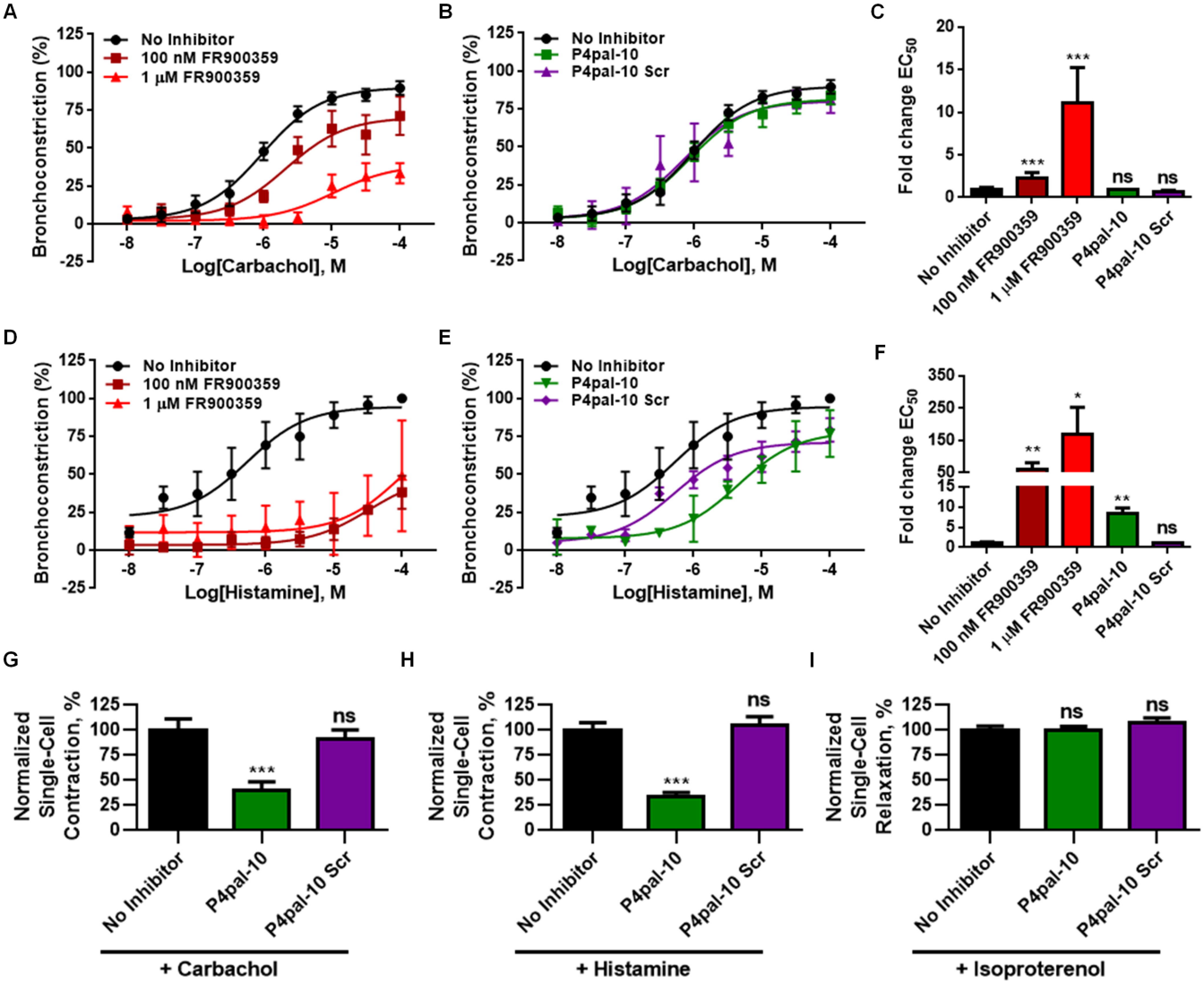
A
No Inhibitor
100 nM FR900359
1 μM FR900359
Bronchoconstriction (%)
Log[Carbachol], M
B
No Inhibitor
P4pal-10
P4pal-10 Scr
Bronchoconstriction (%)
Log[Carbachol], M
C
Fold change EC50
***
***
ns
ns
No Inhibitor
100 nM FR900359
1 μM FR900359
P4pal-10
P4pal-10 Scr
D
No Inhibitor
100 nM FR900359
1 μM FR900359
Bronchoconstriction (%)
Log[Histamine], M
E
No Inhibitor
P4pal-10
P4pal-10 Scr
Bronchoconstriction (%)
Log[Histamine], M
F
Fold change EC50
**
*
**
ns
No Inhibitor
100 nM FR900359
1 μM FR900359
P4pal-10
P4pal-10 Scr
G
Normalized Single-Cell Contraction, %
***
ns
No Inhibitor
P4pal-10
P4pal-10 Scr
+ Carbachol
H
Normalized Single-Cell Contraction, %
***
ns
No Inhibitor
P4pal-10
P4pal-10 Scr
+ Histamine
I
Normalized Single-Cell Relaxation, %
ns
ns
No Inhibitor
P4pal-10
P4pal-10 Scr
+ Isoproterenol

Figure 4